tion for novel antitumor therapy. *In vivo* animal studies have shown that systemic administration of α-GalCer can lead to anti-tumor effects against various tumors (including melanoma, sarcoma, colon carcinoma, and lymphoma) in hepatic and lung metastasis models.[20,21] Intravenous administration of α-GalCer pulsed DCs leads to more potent anti-tumor activities than direct administration of α-GalCer alone in mouse metastatic tumor models.[18,22] Based on the promising results of preclinical studies demonstrating the antitumor potential of α-GalCer, several phase I clinical studies have been done in cancer immunotherapy using intravenous administration of α-GalCer or α-GalCer-loaded DCs, but with limited clinical responses.[23-26] This might partly be because intravenous administered α-GalCer or α-GalCer-loaded DCs may not be delivered efficiently to the tumor site. Although the antitumor effect of α-GalCer has been demonstrated in murine metastatic liver tumor,[20-22,27] no clinical trial against liver cancer has been reported to date. For further development of liver cancer treatment, intrahepatic (i.h.) injection of α-GalCer-loaded DCs, expected to be the most efficient delivery system for tumor lesions, should be tested with respect to inducing effective antitumor therapy.

In this study, we evaluated the antitumor effect of i.h. injection of α-GalCer-pulsed DCs in murine liver tumor. Compared to the conventional peptide-pulsed DC vaccine, we observed effective antitumor effects against not only liver tumor but also disseminated tumor via more efficient activation of innate and acquired immunity in the liver.

Materials and Methods

Mice. Six- to eight-week-old female BALB/c mice were purchased from Shizuoka Experimental Animal Laboratory (Shizuoka, Japan), and maintained in microisolator cages. The animals were handled under aseptic conditions. Procedures were performed according to approved protocol and in accordance with recommendations for the proper care and use of laboratory animals.

Cell Lines and $p53_{232-240}$ Peptide. CMS4 sarcomas ($H\text{-}2^d$) express mutated p53 and present the wild-type $p53_{232-240}$ epitope recognized by $H\text{-}2K^d$-resticted CTL.[28] Colon26, a mouse colon adenocarcinoma cell line, was kindly provided by Dr. Takashi Tsuruo (Institute of Molecular and Cellular Bioscience, University of Tokyo, Tokyo, Japan). These cell lines were maintained in complete media (CM), which is RPMI-1640 medium supplemented with 10% heat-inactivated fetal bovine serum, 100 U/ml penicillin, 100 μg/ml streptomycin, and 10 mM L-glutamine (all reagents from GIBCO/Life Technologies, Grand Island, NY), in a humidified incubator at 5% CO_2 and 37°C.

α-GalCer. Alpha-GalCer was kindly provided by Kirin Brewery (Gunma, Japan) and prepared as described by Kawano et al.[9]

Preparation of α-GalCer-Pulsed DCs or p53 Peptide-Pulsed DCs. Bone marrow derived DCs were generated from BALB/c mice as previously described with minor modification.[29] Briefly, BALB/c bone marrow was cultured in CM supplemented with 1000 U/ml of rmGM-CSF and 1000 U/ml of rmIL-4 (PeproTech EC, London, UK) for 7 days. CD11c+ dendritic cells were isolated from whole bone marrow culture by magnetic cell sorting using MACS (Miltenyi Biotec, Gladbach, Germany) according to the manufacturer's protocol. DCs typically represented >90% of the harvested population of cells based on the morphology and expression of the CD11b, CD11c, CD40, CD80, CD86, and class II MHC antigens (data not shown). On day 7, DCs were added to α-GalCer (100 ng/ml) and cultured for 24 hours to prepare α-GalCer-pulsed DCs (αGCDC). To prepare p53 peptide-pulsed DCs (pepDC), the mouse $p53_{232-240}$ peptide was added to day 7 DCs as described.[28] Alpha-GCDC or pepDC were then washed twice with PBS before i.h. injection of these cells.

Animal Experiments. BALB/c mice were intrahepatically injected with 5×10^5 CMS4 cells and 1×10^6 αGCDC, pepDC, or DCs in a total volume of 100 μl of phosphate-buffered saline (PBS) on day 0. Two weeks after the tumor injection, the livers of the treated mice were removed, and the weight was measured to examine intrahepatic tumor growth. To assess the impact of systemic immunity from i.h. injection of αGCDC, BALB/c mice were injected intrahepatically with 5×10^5 CMS4 cells or Colon26 cells and 1×10^6 αGCDC. On day 28 after i.h. injection, 1×10^6 CMS4 cells or Colon26 cells were injected into the right flank of treated mice. Tumor size was assessed every 3 or 4 days and recorded in square millimeters by determining the product of the largest perpendicular diameters measured using vernier calipers. Data are reported as the average tumor area ± SD.

IFN-γ ELISA. Mice sera were harvested 2 weeks after intrahepatic tumor injection and αGCDC or pepDC treatment, and subjected to mouse IFN-γ ELISA (BD-Pharmingen, San Diego, CA), with lower levels of detection of 31.3 pg/ml.

Cytotoxic Assay. BALB/c mice were treated with an i.h. injection of 1×10^6 αGCDC, pepDC or DCs. After 48 hours, hepatic mononuclear cells (MNCs) were prepared as previously described.[20] To evaluate the cytotoxicity of hepatic NK cells, WST-8 [2-(2-methoxy-4-nitrophenyl)-3-(4-nitrophenyl)-5-(2,4-disulfophenyl)-

2H-tetrazolium, monosodium, salt] assay (Nacalai Tesque, Kyoto, Japan) was performed as described with minor modification.[29] After 24 hours of coculture of hepatic MNC and NK-susceptible YAC-1 target cells at the 5:1 ratio (hepatic MNC:YAC-1 cells) in 96-well plates, 10 μl WST-8 was added to each well and the cells were incubated for another 1 hour. The 450 nm absorbance was measured using a microplate reader (Benchmark, Bio-Rad Laboratories, CA). NK cell cytotoxicity was calculated as described.[29]

CD8+ T Cell Response Against $p53_{232-240}$ Peptide. On day 14 after i.h. injection of CMS4 cells and αGCDC or pepDC, CD8+ T cells were isolated from the spleen cells of treated mice bearing CMS4 liver tumor by using magnetic beads (MACS) and then were cocultured (1×10^5 cells/well) with syngeneic DCs (2×10^4 cells/well) pulsed with or without $p53_{232-240}$ peptide in 96-well tissue culture plate. After 48 hours incubation, the culture supernatant was collected and analyzed for IFN-γ release using specific ELISA kit (BD-Pharmingen).

T Cell and NK Cell Depletion Experiments. On days −6, −1, 5, and 10 after tumor inoculation, mice were injected intraperitoneally with anti-CD4 [GK1.5 hybridoma, American Type Culture Collection (ATCC), Manassas, VA] or anti-CD8 (53-6.72 hybridoma, ATCC) as described.[29] The efficiency of specific subset depletions was validated by flow cytometry analysis of splenocytes using PE-conjugated anti-CD4 and anti-CD8 mAbs (Pharmingen). For NK cell depletion, mice were injected with anti-asialo GM-1 (Wako, Osaka, Japan) on day −1, 5, and 10 after tumor inoculation. The efficiency of NK cell depletion was validated by flow cytometry analysis of splenocytes using PE-conjugated anti-DX5 mAbs (Pharmingen). In all cases, 99% of the targeted cell subset was specifically depleted (data not shown).

Statistical Analysis. The statistical significance of differences between the groups was determined by applying the Student t test or 2-sample *t* test with Welch correction after each group had been tested with equal variance and Fisher's exact probability test. The statistical significance of the differences in more than 2 groups was determined by applying one-way ANOVA. Survival reliability was estimated from the Kaplan-Meier curve, and statistics were analyzed by the log rank test. We defined statistical significance as $P < 0.05$.

Results

Intrahepatic Delivery of αGCDC Is More Therapeutic Than pepDC in the CMS4 Liver Tumor Model. We examined the therapeutic potential of αGCDC or pepDC against CMS4 liver tumor. DCs were generated from bone marrow cells and pulsed with α-GalCer or $p53_{232-240}$ peptide. BALB/c mice were injected intrahepatically with 5×10^5 CMS4 cells and 1×10^6 αGCDC, pepDC, DCs only or PBS. Two weeks after the tumor injection, the livers of the treated mice were removed, and the weight was measured to examine intrahepatic tumor growth. Large CMS4 tumors formed in all mice treated with either PBS or DCs (Fig. 1A). Small CMS4 tumors formed in the liver of pepDC treated mice, with the exception of 1 mouse among the 6 pepDC-treated mice. No tumor formation was observed in the liver of any of the αGCDC-treated mice. The liver weight of the pepDC treatment group tended to be lighter than that of the PBS treatment group, but not with statistical significance. The liver weight of the αGCDC treatment group was significantly lighter than that of the PBS treatment groups (Fig. 1B). The survival rate of the pepDC-treated group was significantly higher than those of the DC-treated or PBS-treated groups ($P < 0.05$) whereas that of the DC-treated group was not significantly different from that of the PBS-treated group. All αGCDC-treated mice survived at 70 days after tumor inoculation, but all pepDC-treated mice died within 35 days (Fig. 1C). These results suggested that the αGCDC treatment has more therapeutic potential against CMS4 liver tumor than conventional pepDC treatment. Therapeutic potential of αGCDC is not unique to CMS4 liver tumor model, because no Colon26 liver tumor was observed in mice treated with αGCDC and the liver weight of αGCDC-treated mice was significantly lighter than that of PBS-treated mice (Fig. 2).

Serum IFN-γ Level and Hepatic NK Cell Activation Are Associated with the Degree of Therapeutic Effect. We next evaluated whether the therapeutic benefits observed in our DC-based treatment regimens were associated with the degree of serum IFN-γ in treated animals. Mice serum was harvested 2 weeks after intrahepatic tumor injection and αGCDC or pepDC treatment, and subjected to mouse IFN-γ ELISA. Serum IFN-γ levels were elevated in αGCDC-treated and pepDC-treated mice, whereas no IFN-γ was detected in PBS-treated mice, mice treated with DCs only, or normal nontreated mice (Fig. 3A). The serum IFN-γ of αGCDC-treated mice was significantly higher than that of pepDC-treated mice,

To examine whether hepatic NK cells were actually activated by i.h. injection of αGCDC or pepDC, we examined the cytotoxic activity of hepatic MNC against YAC-1 cells after i.h. injection of αGCDC or pepDC. The cytotoxic activity of αGCDC-treated mice was significantly stronger than those of pepDC-treated, DC-treated, or PBS-treated mice (Fig. 3B).

These results indicated that i.h. injection of αGCDC in the liver could induce IFN-γ production in treated

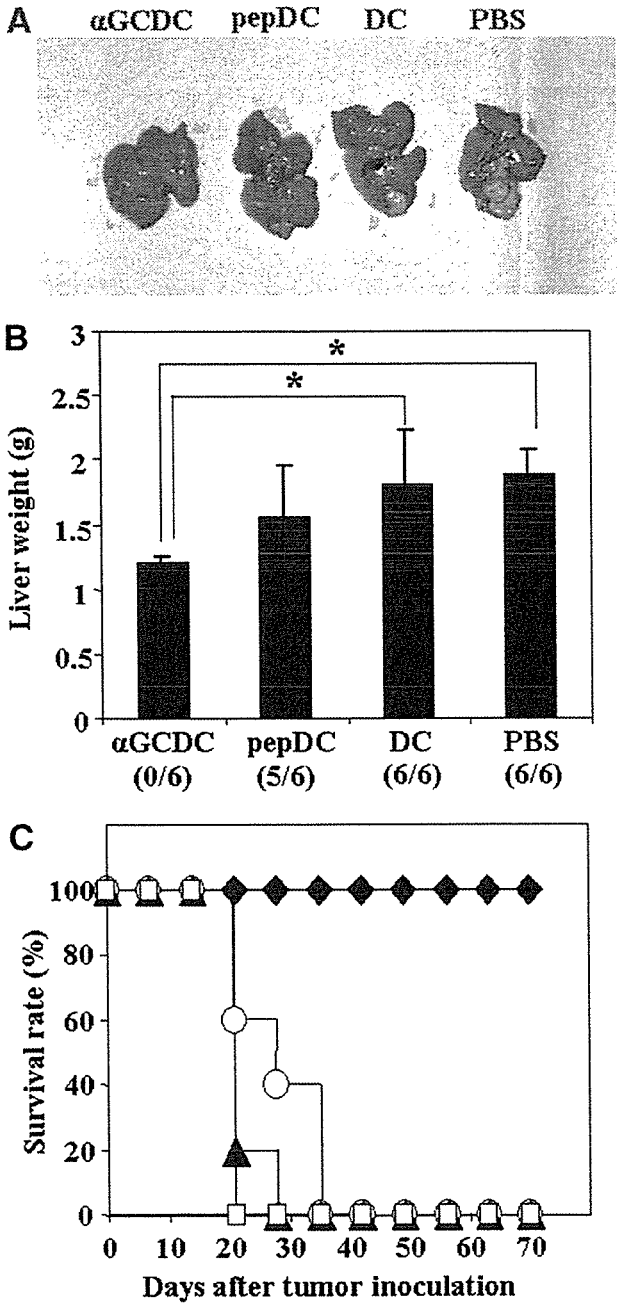

Fig. 1. Improved therapeutic effectiveness of i.h. delivered α-GalCer-pulsed DCs in CMS4 liver tumor model. BALB/c mice were injected intrahepatically with 5×10^5 CMS4 cells and 1×10^6 α-GalCer-pulsed DCs (αGCDC), $p53_{232\text{-}240}$ peptide-pulsed DCs (pepDC), DCs only (DC), or PBS (n = 6 in each treatment group). Two weeks after the CMS4 tumor injection, the livers were removed from all treated mice. (A) Representative liver macroscopic view of each group. (B) Comparison of liver weight of each group. As a control, the mean liver weights of untreated normal mice were 1.11 ± 0.05 g. $*P < 0.05$. In all cases, the fraction of mice bearing liver tumor in each treatment group at 14 days is given in parentheses. (C) Survival curve of mice intrahepatically inoculated with CMS4 cells. CMS4 liver tumor bearing mice were treated with αGCDC (solid diamonds), pepDC (empty circles), DC (solid triangles), or PBS (empty squares) (n = 10 in each treatment group).

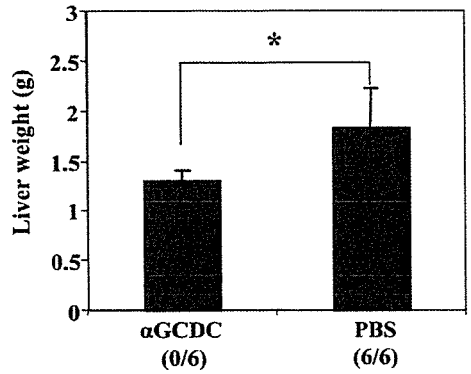

Fig. 2. Improved therapeutic effectiveness of i.h. delivered α-GalCer-pulsed DCs in Colon26 liver tumor model. BALB/c mice were injected intrahepatically with 5×10^5 Colon26 cells and 1×10^6 α-GalCer-pulsed DCs (αGCDC) or PBS (n = 6 in each treatment group). Two weeks after the Colon26 tumor injection, the livers were removed from all treated mice. As a control, the mean liver weights of untreated normal mice were 1.11 ± 0.05 g. Comparison of liver weight of each group. $*P < 0.05$. In all cases, the fraction of mice bearing liver tumor in each treatment group at 14 days is given in parentheses.

mice and efficiently activate hepatic NK cells, suggesting that there may be an association between IFN-γ production or NK cell activation and the degree of therapeutic effects observed in this system.

Depletion of NK Cells Abolishes the Antitumor Effect of αGCDC. To verify that the therapeutic benefit of αGCDC-based regimen in the CMS4 liver tumor model was T cell-dependent and NK cell-dependent, we performed T cell subset depletion and NK cell depletion studies (Fig. 4). NK cell depletions significantly inhibited the therapeutic efficacy of i.h. injections with αGCDC ($P < 0.05$ versus NK cell-depleted mice). In contrast, neither CD4+ nor CD8+ T cell depletions inhibited the therapeutic efficacy of i.h. injection with αGCDC. These results suggested that NK cells, but neither CD8+ nor CD4+ T cells, play critical roles in the antitumor effect against mouse liver tumor.

$p53_{232\text{-}240}$ Peptide-Specific CTLs Are Generated After DC Treatment of Liver Tumor. We next evaluated whether $p53_{232\text{-}240}$ peptide-specific CTLs were generated after treatment of liver tumor by DC treatment. CD8+ T cells were isolated from the spleen cells of treated mice and then cocultured with syngeneic DCs pulsed with $p53_{232\text{-}240}$ peptide strongly expressed on CMS4 cells. The $p53_{232\text{-}240}$ peptide-specific IFN-γ production of CD8+ T cells differed significantly among the treatment groups (Fig. 5). CD8+ T cells from mice treated with αGCDC produced higher levels of the Th-1 associated cytokine IFN-γ in response to $p53_{232\text{-}240}$ peptide than CD8+ T cells obtained from mice treated with any other DC-based vaccine or with

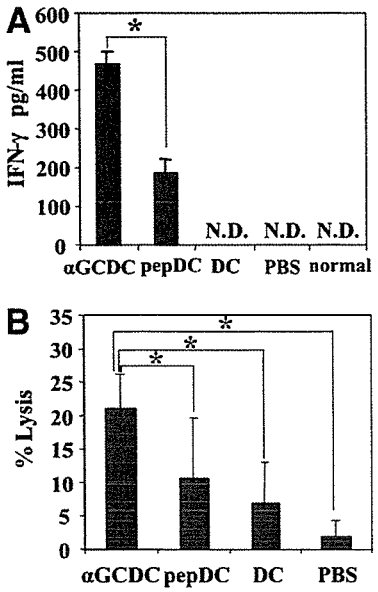

Fig. 3. Increase in serum IFN-γ levels and activation of hepatic NK cells in mice treated with αGCDC. (A) Mice sera were harvested two weeks after intrahepatic CMS4 tumor injection and treatments of αGCDC, pepDC treatment, DC only, or PBS, and subjected to IFN-γ ELISA. Naïve mice (normal) were used as controls. Cytokine levels are reported in picograms per milliliter (mean ± SD of triplicate samples). Similar results were obtained in 2 independent experiments. N.D., not detected. $*P < 0.05$. (B) BALB/c mice were treated with an i.h. injection of 1×10^6 αGCDC, pepDC, DC only, or PBS. After 48 hours, hepatic mononuclear cells were isolated from the liver to evaluate the cytotoxicity against YAC-1 cells at 5:1 effector/target cells ratio. Similar results were obtained in 2 independent experiments. $*P < 0.05$.

PBS only, suggesting that strong $p53_{232\text{-}240}$ peptide-specific CTLs were generated by αGCDC treatment of the liver tumor.

Systemic Therapeutic Antitumor Immunity Is Induced by i.h. Injection with αGCDC. Because strong anti-CMS4 CTL response was generated in αGCDC-treated animals, we next chose to analyze whether treatment of a CMS4 lesion in the liver would affect the growth of rechallenged CMS4 tumors. BALB/c mice were intrahepatically injected with CMS4 tumors and αGCDC. After 28 days, 1×10^6 CMS4 cells or Colon26 cells were injected subcutaneously in the right flank. The subcutaneous CMS4 tumors in mice receiving the αGCDC regimen were completely rejected in all mice (Fig. 6A). The growth of subcutaneous Colon26 tumor in αGCDC-treated mice was not inhibited, suggesting that CMS4 specific antitumor immunity could be induced (Fig. 6B) by αGCDC treatment. Acquired immune responses induced by αGCDC is not unique to CMS4 tumor model, because the subcutaneous tumor growth of Colon26 cells (Fig. 6D), but not CMS4 cells (Fig. 6C), were also significantly inhibited in mice that had been

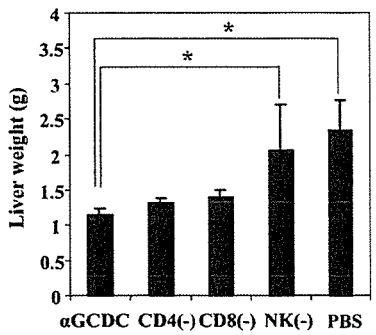

Fig. 4. Dependence of antitumor efficacy of i.h. αGCDC delivery on NK cells, not on CD4+ or CD8+ T cells. To prove that the therapeutic benefit of αGCDC-based regimen in the CMS4 liver tumor model is T cell-dependent and NK cell-dependent, the liver weights of αGCDC treated mice with $CD4^+$ (CD4(-)) and $CD8^-$ (CD8(-)) T cell subset or NK cell (ASGM1) depletion or without depletion (αGCDC) were shown. The liver weights of mice treated with PBS were also shown. As a control, the mean liver weights of untreated normal mice were 1.11 ± 0.05 g. Ab-mediated *in situ* depletion of NK cells, but not $CD4^+$ or $CD8^+$ T cells, markedly reduced the therapeutic efficacy of αGCDC therapy ($n = 6$ in each treatment group). $*P < 0.05$ versus αGCDC.

protected Colon26 liver tumor by i.h. injection of αGCDC.

Discussion

Tumor associated antigen derived peptide-pulsed DCs-based vaccine have been reported in various mouse tumor models,[30,31] and clinical applications of peptide-pulsed DCs have been tried with various cancer patients.[3,32-34] However, although tumor-specific T cells were promoted by vaccination in most patients, objective clinical responses have thus far only been observed in a

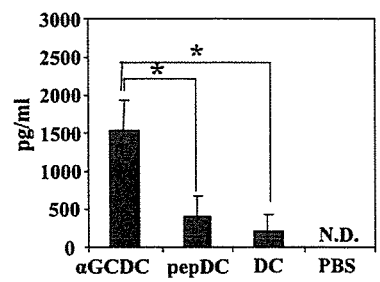

Fig. 5. Evaluation of $p53_{232\text{-}240}$ peptide specific CD8+ CTL in responder mice. CD8+ T cells were isolated from the spleen of mice 14 days after i.h. injection with DCs (αGCDC, α-GalCer pulsed DCs; pepDC, $p53_{232\text{-}240}$ peptide pulsed DCs; DC, DCs only; PBS, control) and CMS4 cells. IFN-γ production from CD8+ T cells against $p53_{232\text{-}240}$ peptide was measured by ELISA (results in picograms per milliliter; mean ± SD of triplicate samples). Syngeneic DCs pulsed with $p53_{232\text{-}240}$ peptide served as the antigen-presenting cells. IFN-γ production from CD8+ T cells against peptide-unpulsed syngeneic DCs served as negative control, and this value was subtracted from all experimental determinations to determine $p53_{232\text{-}240}$ peptide specific IFN-γ production. Similar results were obtained in two independent experiments. N.D., not detected. $*P < 0.05$.

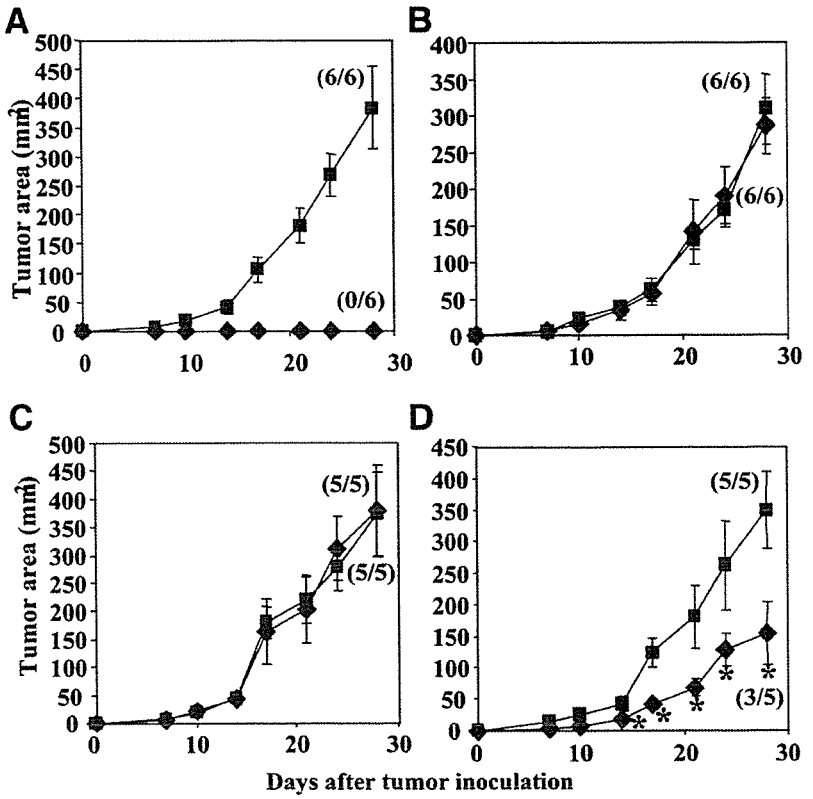

Fig. 6. Alpha-GCDC-based intrahepatic therapy results in the development of systemic anti-tumor immunity that protects distal tumor rechallenge. On day 0, BALB/c mice were injected intrahepatically with αGCDC and either CMS4 tumors (A, B, n = 6 in each treatment group)or Colon26 tumors (C, D, n = 5 in each treatment group). Twenty-eight days after treatment, mice were challenged subcutaneously with 1×10^6 CMS4 cells (A, C) or Colon26 cells (B, D) injected into the right flank. As a control, naïve mice were challenged with 1×10^6 CMS4 cells (A, C) or Colon26 cells (B, D).The fraction of mice bearing a tumor in each treatment group at day 28 is indicated in parentheses. Tumor size was expressed as the mean tumor size of only those mice bearing a tumor. αGCDC treated mice (solid diamonds); naive mice (solid squares). Each data point represents the mean tumor size ± SD. *$P < 0.05$. versus naive mice.

minority of treated individuals. A normal liver contains lymphocytes that are usually enriched with NK and NKT cells; i.e., 25% NK cells and 30% NKT cells in contrast to peripheral blood that contains only 10% NK and 5% NKT cells.[12,13] Recently, DCs have been implicated in the activation of NKT and NK cells in both mice and humans,[4-6,9-11,23,35] suggesting that activation of many innate immune cells in the liver by a DC-based vaccine would be promising for treating liver tumor. We hypothesize that i.h. injection of α-GalCer-pulsed DC can efficiently activate abundant innate immune cells in the liver and elicit effective innate and acquired immunity against liver tumor. Our results demonstrated that i.h. injection with αGCDC resulted in complete rejection of CMS4 liver tumors with prolonged survival of tumor-bearing mice whereas injection with pepDC did not. These results suggested the efficacy of i.h. injection of αGCDC for treating liver cancer and the superiority of αGCDC treatment over conventional pepDC treatment. Intrahepatic injection of αGCDC also revealed a strong antitumor effect in the Colon26 liver tumor model. Although DCs pulsed with both α-GalCer and peptide (αGC-pepDC) would be expected to provide a better therapy index, the therapeutic potential of αGC-pepDC was found to be similar with that of αGCDC in the CMS4 liver tumor model (Tatsumi T et al., unpublished data). These findings suggest that i.h. delivery of αGCDC may optimally promote antitumor effects in the mouse liver tumor microenvironment.

We have shown that serum IFN-γ was detected in αGCDC-treated and pepDC-treated mice and that serum IFN-γ levels in αGCDC-treated mice were significantly higher than in pepDC-treated mice. Zitvogel et al. reported that the antitumor effects of DC-based vaccination were dependent on the production of Th1-associated cytokines such as IFN-γ, tumor necrosis factor-α, and IL-12.[36] Therefore, enhanced IFN-γ production resulting from injection of αGCDC or pepDC into liver tumor may also play an important role in the antitumor activity in vivo. Our results also suggested that αGCDC treat-

ment in the liver could induce stronger antitumor immunity than pepDC treatment.

Efficient activation of abundant NKT cells and NK cells in the liver might be important in an antitumor effect against liver tumor. We and others have previously reported that sequential activation of NKT cells and NK cells could be observed in the liver after α-GalCer administration and that most NKT cells had disappeared from the liver within 12 hours of α-GalCer administration.[20,37] Thus, the activated NK cells mainly play critical roles in the antitumor effect of disseminated liver tumor.[20] We found that the NK cell activity of αGCDC-treated mice were significantly stronger than those of pepDC-treated, DC-treated, or PBS-treated mice. These findings offer evidence that intrahepatic injection of DCs activate hepatic NK cells and that αGCDC may activate liver abundant NK cells more efficiently than pepDC, which might be associated with the therapeutic outcomes of these treatments in liver tumors.

In this study, the depletion of NK cells, but not CD4+ or CD8+ T cells, diminished the antitumor effect against liver tumor by α-GalCer pulsed DCs. These results suggested that only NK cells play a critical role in eradication of mouse liver tumor by i.h. injection of αGCDC and that neither CD4+ nor CD8+ T cells play critical roles in the early phase of the eradication of liver tumor cells. However, our following results demonstrated that strong systemic acquired immunity could be generated after early eradication of liver tumor by treatment with αGCDC. These results suggested that NK cells activated by αGCDC might be the main effector cells in the early eradication of liver tumor cells and that liver tumor-derived tumor antigens are taken up by dedicated professional antigen-presenting cells in the liver, which might generate prolonged liver tumor antigen-specific acquired immunity.

Subsequent analyses revealed that CD8+ T cells isolated from mice treated with i.h. injection of αGCDC or pepDC in liver tumors secrete IFN-γ in response to $p53_{232-240}$ peptide strongly expressed on CMS4 cells when presented by syngeneic DCs *in vitro*. The IFN-γ level of CD8+ T cells from αGCDC-treated mice was much higher than that from pepDC-treated mice. Mayordomo et al. reported that immunization of $p53_{232-240}$ peptide-pulsed DCs induced peptide-specific CTL in immunized mice that showed cytolytic activity against CMS4, p53 overexpressing cells, and that $p53_{232-240}$ peptide-pulsed DC vaccine offered protection against CMS4 tumor challenge in mice.[28] These results suggested the therapeutic potential of $p53_{232-240}$ peptide-based DCs vaccine in the CMS4 tumor model. Our current data revealed that i.h. injection of αGCDC to liver tumors generated $p53_{232-240}$ peptide-specific CTL more efficiently than that of pepDC. The activation of NKT cells was associated with an expansion of antigen-specific CTL, as might be expected if the DCs that matured *in vivo* in response to NKT cells were capturing antigens.[38-41] In a clinical study, Chang et al. reported that increases of antigen-specific memory T cells were observed in cancer patients treated with α-GalCer-pulsed dendritic cells.[26] Our results suggested that the activation of hepatic NK cells in the liver might be associated with the efficiency of generation of tumor antigen-specific CTL. We believe that injection of αGCDC into the liver more efficiently activates innate immune cells, NKT cells and NK cells, followed by generation of tumor antigen-specific CTL than injection of pepDC.

Additional experiments using subcutaneous rechallenge with tumor demonstrated that i.h. αGCDC treatment of liver tumors not only blocked treated CMS4 liver tumor progression but offered complete protection against "recurrence" of the same tumor at a distant site. In contrast, Colon26 rechallenge tumor was not inhibited in the treated mice, suggesting that CMS4-specific immunity was generated after liver tumor treatment. These results were consistent with the activation of acquired immunity evaluated by IFN-γ secretion from CD8+ T cell in response to $p53_{232-240}$ peptide. Intrahepatic αGCDC treatment of Colon26 liver tumor also led to resistance to subsequent Colon26 challenge but not to CMS4 challenge. These data supported that i.h. αGCDC injection generally induced acquired immunity after rejection of original liver tumors. Taken together, we believe that i.h. αGCDC treatment of liver tumors offers the optimal therapeutic treatment for both local liver tumor and distant metastatic tumor.

In spite of recent progress and early successes reported for DC-based cancer immunotherapies, there remains significant room for improvement in these regimens, especially with respect to advanced liver cancer. The liver is the most common site of metastasis of gastrointestinal cancers (i.e. colorectal cancer, gastric cancer and pancreatic cancer). Thus, new therapeutic approaches of DC-based immunotherapy for advanced liver tumor need to be developed. Recently, percutaneous liver tumor ablation methods, radiofrequency ablation (RFA) therapy, and ethanol injection therapy (PEIT) have become well-established in hepatocellular carcinoma treatment. This encourages gastroenterologists to apply i.h. injection-immunotherapy to liver tumor treatment. We show here that i.h. injection of α-GalCer-pulsed DCs has greater antitumor efficacy than that of tumor antigen-derived peptide-pulsed DCs in liver cancer treatment and that i.h. injection of α-GalCer pulsed DCs into liver tumor results

in the coordinated activation of both innate and acquired immunity in the liver, leading to superior antitumor efficacy. These findings indicate that the use of i.h. delivery of α-GalCer-pulsed DCs might represent a particularly promising approach to suppressing tumor growth and promoting regression of metastatic lesions in liver cancer patients.

Acknowledgment: The authors thank the Pharmaceutical Research Laboratories, Kirin Brewery (Gunma, Japan) for providing the α-galactosylceramide.

References

1. Steinman RM. The dendritic cell system and its role in immunogenicity. Annu Rev Immunol 1991;9:271-296.
2. Hart DN. Dendritic cells: unique leukocyte populations which control the primary immune response. Blood 1997;90:3245-3287.
3. O'Neill DW, Adams S, Bhardwaj N. Manipulating dendritic cell biology for the active immunotherapy of cancer. Blood 2004;104:2235-2246.
4. Fernandez NC, Lozier A, Flament C, Ricciardi-Castagnoli P, Beller D, Suter M, et al. Dendritic cells directly trigger NK cell functions: cross-talk relevant in innate anti-tumor immune responses in vivo. Nat Med 1999; 5:405-411.
5. Gerosa F, Baldani-Guerra B, Nisii C, Marchesini V, Carra G, Trinchieri G. Reciprocal activating interaction between natural killer cells and dendritic cells. J Exp Med 2002;195:327-333.
6. Ferlazzo G, Tsang ML, Moretta L, Melioli G, Steinman RM, Munz C. Human dendritic cells activate resting NK cells and are recognized via the NKp30 receptor by activated NK cells. J Exp Med 2002;195:343-351.
7. Piccioli D, Sbrana S, Melandri E, Valiante NM. Contact-dependent stimulation and inhibition of dendritic cells by natural killer cells. J Exp Med 2002;195:335-341.
8. Miller G, Lahrs S, Dematteo RP. Overexpression of interleukin-12 enables dendritic cells to activate NK cells and confer systemic antitumor immunity. FASEB J 2003;17:728-730.
9. Kawano T, Cui J, Koezuka Y, Toura I, Kaneko Y, Motoki H, et al. CD1d-restricted and TCR-mediated activation of Vα14NKT cells by glycosylceramides. Science 1997;278:1626-1629.
10. Kawano T, Cui J, Koezuka Y, Toura I, Kaneko K, Sato H, et al. Natural killer-like nonspecific tumor cell lysis mediated by specific ligand-activated Vα14NKT cells. Proc Natl Acad Sci U S A 1998;95:5690-5693.
11. Kitamura H, Iwakabe K, Yahata T, Nishimura S, Ohta A, Ohmi S, et al. The natural killer T (NKT) cell ligand α-galactosylceramide demonstrates its immunopoteniating effect by inducing interleukin (IL)-12 production by dendritic cells and IL-12 receptor expression on NKT cells. J Exp Med 1999;189:1121-1128.
12. Doherty DG, O'Farrelly C. Innate and adaptive lymphoid cells in human liver. Immunol Rev 2000;174:5-20.
13. Mehal WZ, Azzaroli F, Crispe IN. Immunology of the healthy liver: Old questions and new insights. Gastroenterology 2001;120:250-260.
14. Ladhams A, Schmidt C, Sing G, Butterworth L, Fielding G, Tesar P, et al. Treatment of non-resectable hepatocellular carcinoma with autologous tumor-pulsed dendritic cells. J Gastroenterol Hepatol 2002;17:889-896.
15. Iwashita Y, Tahara K, Goto S, Sasaki A, Kai S, Seike M, et al. A phase I study of autologous dendritic cell-based immunotherapy for patients with unresectable primary liver cancer. Cancer Immunol Immunother 2003;52: 155-161.
16. Chi KH, Liu SJ, Li CP, Kuo HP, Wang YS, Chao Y, et al. Combination of conformal radiotherapy and intratumoral injection of adoptive dendritic cell immunotherapy in refractory hepatoma. J Immunother 2005;28:129-135.
17. Lee WC, Wang HC, Hung CF, Huang PF, Lia CR, Chen MF. Vaccination of advanced hepatocellular carcinoma patients with tumor lysate-pulsed dendritic cells: a clinical trial. J Immunother 2005;28:496-504.
18. Fujii S, Shimizu K, Kronenberg M, Steinman RM. Prolonged IFN-γ-producing NKT response induced with alpha-galactosylceramide-loaded DCs. Nat Immunol 2002;3:867-874.
19. Gonzalez-Aseguinolaza G, de Oliveira C, Tomaska M, Hong S, Bruna-Romero O, Nakayama T, et al. α-Galactosylceramide-activated Vα 14 natural killer T cells mediate protection against murine malaria. Proc Natl Acad Sci U S A 2000;97:8461-8466.
20. Miyagi T, Takehara T, Tatsumi T, Kanto T, Suzuki T, Jinushi M, et al. CD1d-mediated stimulation of natural killer T cells selectively activates hepatic natural killer cells to eliminate experimentally disseminated hepatoma cells in murine liver. Int J Cancer 2003;106:81-89.
21. Nakagawa R, Motoki K, Ueno H, Iijima R, Nakamura H, Kobayashi E, et al. Treatment of hepatic metastasis of the colon26 adenocacinoma with an α-galactosylceramide, KRN7000. Cancer Res 1998;58:1202-1207.
22. Toura I, Kawano T, Akutsu Y, Nakayama T, Ochiai T, Taniguchi M. Inhibition of experimental tumor metastasis by dendritic cells pulsed with α-galactosylceramide. J Immunol 1999;163:2387-2391.
23. Nieda M, Okai M, Tazbirkova A, Lin H, Yamaura A, Ide K, et al. Therapeutic activation of Vα24+Vβ11+NKT cells in human subjects results in highly coordinates secondary activation of acquired and innate immunity. Blood 2004;103:383-389.
24. Giaccone G, Punt CJ, Ando Y, Ruijter R, Nishi N, Peters M, et al. A phase I study of the natural killer T-cell ligand α-galactosylceramide (KRN7000) in patients with solid tumors. Clin Cancer Res 2002;8:3702-3709.
25. Ishikawa A, Motohashi S, Ishikawa E, Fuchida H, Higashino K, Otsuji M, et al. A phase I study of α-galactosylceramide (KRN7000)-pulsed dendritic cells in patients with advanced and recurrent non-small cell lung cancer. Clin Cancer Res 2005;11:1910-1917.
26. Chang DH, Osman K, Connolly J, Kukreja A, Krasovsky J, Pack M, et al. Sustained expansion of NKT cells and antigen-specific T cells after injection of α-galactosyl-ceramide loaded mature dendritic cells in cancer patients. J Exp Med 2005;201:1503-1517.
27. Chiodoni C, Stoppacciaro A, Sangaletti S, Gri G, Cappetti B, Koezuka Y, et al. Different requirements for α-galactosylceramide and recombinant interleukin-12 antitumor activity in the treatment of C-26 colon carcinoma hepatic metastases. Eur J Immunol 2001;31:3101-3110.
28. Mayordomo JI, Loftus DJ, Sakamoto H, De Cesare CM, Appasamy PM, Lotze MT, et al. Therapy of murine tumors with p53 wild-type and mutant sequence peptide-based vaccines. J Exp Med 1996;183:1357-1365.
29. Tatsumi T, Huang J, Gooding WE, Gambotto A, Robbins PD, Vujanovic NL, et al. Intratumoral delivery of dendritic cells engineered to secrete both interleukin(IL)-12 and IL-18 effectively treats local and distant disease in association with broadly reactive Tc1-type immunity. Cancer Res 2003; 63:6378-6386.
30. Porgador A, Snyder D, Gilboa E. Induction of antitumor immunity using bone marrow-generated dendritic cells. J Immunol 1996;156: 2918-2926.
31. Mayordomo JI, Zorina T, Storkus WJ, Zitvogel L, Celluzzi C, Falo LD Jr, et al. Bone marrow-derived dendritic cells pulsed with synthetic tumor peptide elicits protective and therapeutic antitumor immunity. Nat Med 1995;12:1297-1302.
32. Hsu FJ, Benike C, Fagnoni F, Liles TM, Czerwinski D, Taidi B, et al. Vaccination of patients with B-cell lymphoma using autologous antigen-pulsed dendritic cells. Nat Med 1996;2:52-58.
33. Nestle FO, Alijagic S, Gilliet M, Sun Y, Grabbe S, Dummer R, et al. Vaccination of melanoma patients with peptide- or tumor lysate-pulsed dendritic cells. Nat Med 1998;4:328-332.
34. Salgaller ML, Tjoa BA, Lodge PA, Ragde H, Kenny G, Boynton A, et al. Dendritic cell-based immunotherapy of prostate cancer. Crit Rev Immunol 1998;18:109-119.
35. Ferlazzo G, Munz C. NK cell compartments and their activation by dendritic cells. J Immunol 2004;172:1333-1339.
36. Zitvogel L, Mayordomo JI, Tjandrawan T, DeLeo AB, Clarke MR, Lotze MT, et al. Therapy of murine tumors with tumor peptide-pulsed dendritic cells: Dependence on T cells, B7 costimulation, and T helper cell 1-associated cytokines. J Exp Med 1996;183:87-97.

37. Osman Y, Kawamura T, Naito T, Takeda K, Van Kaer L, Okumura K, et al. Activation of hepatic NKT cells and subsequent liver injury following administration of α-galactosylceramide. Eur J Immunol 2000;30:1919-1928.
38. Fujii S, Shimizu K, Smith C, Bonifaz L, Steinman RM. Activation of natural killer T cells by α-galactosylceramide rapidly induces the full maturation of dendritic cells in vivo and thereby acts as an adjuvant for combined CD4 and CD8 T cell immunity to a coadministered protein. J Exp Med 2003;198:267-279.
39. Fujii S, Liu K, Smith C, Bonito AJ, Steinman RM. The linkage of innate to adaptive immunity via maturing dendritic cells in vivo requires CD40 ligation in addition to antigen presentation and CD80/86 costimulation. J Exp Med 2004;199:1607-1618.
40. Hermans IF, Silk JD, Gileadi U, Salio M, Mathew B, Ritter G, et al. NKT cells enhance CD4+ and CD8+ T cells responses to soluble antigen in vivo through direct interaction with dendritic cells. J Immunol 2003;171: 5140-5147.
41. Nishimura T, Kitamura H, Iwakabe K, Yahata T, Ohta A, Sato M, et al. The interface between innate and acquired immunity: glycolipid antigen presentation by CD1d-expressing dendritic cells to NKT cells induces the differentiation of antigen-specific cytotoxic T lymphocytes. Int Immunol 2000;12:987-994.

9. 肝癌免疫療法

大阪大学大学院医学系研究科消化器内科学助教授　竹原徹郎
同　消化器内科学教授　林　紀夫

key words　cytokine, IFNα, adoptive immunotherapy, dendritic cell, AFP-derived peptide

動　向

肝癌は限局した病変であれば肝切除や内科的ablation治療が可能であり，肝予備能および技術的な問題が充分にクリアされ，安全なマージンをとって切除・焼灼することができれば，根治的な治療効果を得ることができる．しかし，肝癌は時間的あるいは空間的に多発性を示すという生物学的な特徴があり，このことが肝癌の治療をきわめて難しいものにしている．肝両葉に多発する癌に対しては，局所治療は無効である．このような場合，肝動脈塞栓術や抗癌剤の動注などが考慮されるが，治療効果には限界がある．また，肝癌はたとえ局所治療に成功しても，異所再発をきたすことが多く，再発抑止法の確立が急務の課題となっている．したがって，進行肝癌の予後を改善し，局所治療後の無再発生存を向上させるためには，新たな視点での全肝治療法の開発が必要であり，このような背景から肝癌に対する免疫治療に期待が高まっている．

癌の免疫治療の歴史は非特異的なものから特異的なものへ，メカニズムの不明なものから明確なものへと進化してきている．生体の免疫応答を全般的に活性化する試みは，菌体成分による免疫賦活療法からサイトカインの利用へと進み，LAK (lymphokine-activated killer cell) による養子免疫治療は腫瘍特異的なTIL (tumor-infiltrating lymphocyte) を用いた方法へ，さらに，非特異的な免疫賦活は樹状細胞や腫瘍特異的抗原を用いたより特異的な治療へと変化してきている．また，従来から免疫賦活に用いられてきた菌体成分が実はToll様レセプターのリガンドであり，これが樹状細胞の成熟をうながすことにより，先天免疫あるいは獲得免疫を活性化することが明らかになり，このような方法の現代的な意味での見直しも行われている．肝癌に対してもサイトカイン治療，養子免疫治療，樹状細胞治療，腫瘍抗原ペプチド療法の各方面において，前臨床研究の成果に基づいて臨床試験が行われており一定の効果が報告されるようになってきている[1-3]．

A. サイトカイン治療

非特異的に免疫系全般の活性化をはかる方策として，先天免疫や獲得免疫を制御する種々のサイトカインの効果が検討されている．

進行肝癌に対するIFNα単独治療については1980年代から1990年代にかけていくつかの報告があるが，有効であるという報告とそれを否定する報告が混在している．最近，Llovetら[4]は58人の進行肝癌例に対して，IFNα-2b (3MU)

を1年間投与する場合と保存的な治療をする場合の効果についての無作為比較試験を行っている．彼らはIFNαの投与は副作用中止率も高く，1年および2年生存率において，対照群と有意差がなかったと結論している．一方，Kuboら[5]はC型肝炎ウイルスの感染を基礎疾患とする30例の肝癌切除患者を無作為に2群に振り分け，15例に対してIFNα（6MU）の2年間投与を行い，対照15例との間での肝癌の再発率を検討している．それによると，IFNα治療群からの肝癌の発生が5例，対照群からは12例であり，IFNα投与群において有意に発癌率が低かったと報告している．IFNαの投与が画像上認識されない微小な肝癌に対して治療効果があるのか，HCV感染を基盤とした新規の再発を抑制しているのかは明らかではないが，肝癌切除後のアジュバント治療としては，無再発生存に寄与することが示唆されている．

このように進行肝癌に対するIFNαの単独治療については限界があることから，他の抗癌剤との併用治療についての検討がなされている．パイロットスタディにおいてMTX＋5-FU＋CDDP＋IFNα[6]，CDDP＋DXR＋5-FU＋IFNα[7]　の併用治療効果が報告されている．これらの治療法はある程度の奏効率が報告されているものの，副作用も強く忍容性が低いことが問題となっている[8]．このようなIFNα併用化学療法のなかで5-FUがキードラッグであることが認識されるようになり，IFNαと5-FUの併用治療法が，進行肝癌の約半数において腫瘍縮小効果が得られることが報告されている[9-11]．最近，38例の進行肝癌を無作為に2群に割付け，5-FU＋IFNα治療と5-FU単独治療の無作為比較試験が行われた．併用群の奏効率が26%，単独治療が11%であり，両群間に有意差はなかったが，累積生存率では併用治療群が有意に良好であったと報告されている．5-FUとIFNαの併用治療効果は腫瘍細胞に対する直接作用が強調されているが[10]，IFNαにはNK細胞活性化能などの多彩な免疫賦活作用があり[12]，進行肝癌に対しても抗癌剤と併用することによりIFNα免疫治療が有効である可能性があると考えられる．

その他のサイトカインとして，Lygidakisら[13]はIL-2とIFNγを抗癌剤と併用する効果について検討している．Stage III～IVの肝癌のうち70%に腫瘍の縮小とAFP値の低下が得られたと報告している．Reinischら[14]は15例の進行肝癌に対してIFNγとGM-CSFとの併用治療法を行い，1例に腫瘍縮小効果があったとしている．

サイトカイン単独による肝癌治療については，再発予防を目的にしたIFNαによるアジュバント治療効果が示唆される以外は，進行癌に対する有効性は示されていない．進行肝癌に対しては化学療法剤との併用を行うことにより，治療効果を上昇させる可能性があると考えられる．

B. 養子免疫治療

生体内で抗腫瘍効果を示す免疫細胞はT細胞やNK細胞である．このようなエフェクター細胞を体外に取り出して活性化しこれを生体に戻して抗腫瘍効果を期待する治療法を養子免疫療法とよんでいる．1980年代中頃にRosenbergら[15]が進行癌患者（肝癌を含まない）を対象に臨床応用した免疫治療法である．我々は治療不能肝癌患者を対象に自己のLAK細胞を週2回4週間にわたってIL-2とともに肝動脈に注入するパイロットスタディを行い，奏効例があることを報告した[16]．最近，Takayamaら[17]は肝癌切除後の患者に対して，末梢血リンパ球を取り出し，これをIL-2，OKT3で刺激し，これを戻すことにより再発率が低下するかどうかを無作為化比較試験で検討している．それによると，無再発生存率は免疫群が対照群に比べて有意に良好であり，再発リスクが41%低下したと報告している．その後，活性化T

リンパ球を用いた肝癌切除後の肝動注免疫療法の有効性も報告されている[18].

C. 樹状細胞治療

樹状細胞（DC）は生体内で最も強力な抗原提示細胞であり，獲得免疫の形成に必須の役割を担っている．また，DCはNK細胞やNKT細胞の活性化能もあり，先天免疫の制御においても重要な役割をもっている．DCは流血中にはきわめて微量にしか存在しないが，末梢血単球をGM-CSFやIL-4存在下に約1週間培養することにより，分化誘導することが可能である．このようにして誘導したDCは未成熟な表現型を示すが，これをLPSやTNFαで刺激することにより成熟させることができる．一般に未成熟DCは貪食能が高いが抗原提示能や遊走能が低く，また成熟DCは貪食能は低いが抗原提示・遊走能が高い．DCのex vivo誘導には時間がかかり，またヒトでの安全性が必ずしも保障されていない薬剤を用いる必要があるなどの問題があったが，最近，我々はこれらの問題を克服した新規の誘導法を開発し，進行癌に対する免疫治療に用いている[19].

肝癌に対するDC治療としてはすでに3つのパイロットスタディの結果が報告されている．Ladhamsら[20]は，未成熟DCを自己の腫瘍細胞と混合刺激し，これを2例の肝癌患者に皮下接種した．重篤な副作用の出現はなく1例において，臨床経過が改善されたと報告している．Iwashitaら[21]は未成熟DCを腫瘍細胞lysateでパルスし，その後TNFαを用いて成熟誘導し，これを10例の切除不能肝癌患者の鼠径リンパ節に投与した．2例に軽度の腫瘍マーカーの低下と，1例に腫瘍の縮小を認め，重篤な合併症を認めた症例はなかったと報告している．彼らは同時にDCをマーカーとしてKLHで刺激し，7例においてDTH陽性になったことを示し，進行肝癌患者においてDCが明らかに特異免疫応答を誘導し得ることを示した．Stiftら[22]はTNFαで分化誘導したDCに腫瘍lysateをパルスし，これを2例の進行肝癌症例に投与している．明確な抗腫瘍効果は認められなかったと報告している．

DCを用いた抗腫瘍効果の限界を克服する1つの方法として，Tatsumiら[23]はIL-12の併用効果について検討しており，IL-12存在下においてDCの抗腫瘍効果が増強することを報告している．このような動物実験の結果を受けてIL-12で遺伝子改変を行ったDCの抗腫瘍効果についての検討がなされている．Mazzoliniら[24]はIL-12発現アデノウイルスをトランスフェクションしたDCを肝腫瘍に直接注入し，その安全性と効果について検討した．それによると，安全性に関しては問題がなかったが，期待された抗腫瘍効果は認められなかった．この1つの機序として腫瘍細胞がIL-8を分泌することにより，投与したDCが腫瘍局所にトラップされてしまう可能性が示唆されている[25]．DCは2次リンパ節においてT細胞を活性化することから，DCをリンパ節に直接注入する方法が検討される必要がある．

以上のように，DCを用いた肝癌に対する免疫治療法は進行肝癌を対象としたパイロットスタディが中心であるが，明確な治療効果は示されていない．今後，投与経路の工夫やより強力なDCの使用などの検討が必要である．また，進行癌症例に対する検討だけでなく，根治後の補助療法における意義などの検討も必要である．

D. 腫瘍ペプチドワクチン治療

肝癌は種々の腫瘍抗原を発現しており，患者末梢血中にはAFP[26]，NY-ESO-1[27]，MAGE-Aファミリー[28]，Glypican-3[29]などに対して特異的に反応するT細胞が存在することが知られている．このような知見を背景に，不活化した腫瘍細

胞や腫瘍抗原特異ペプチドを用いた肝癌に対する獲得免疫誘導の治療効果について臨床的な検討が行われている.

Kuangら[30]は，肝癌治癒切除54例を自己フォルマリン固定腫瘍ワクチン投与群と非投与群に無作為に割付けた．観察期間中央値15カ月の時点で，無再発生存は投与群が対照群に比べ有意に良好であった．再発リスクが81%低下したとしている.

Butterfieldら[31]はAFPを標的としたペプチド療法の可能性について検討している．彼らはAFPに対する特異的T細胞応答を誘導するHLA-A*0201拘束性のペプチド領域を4カ所同定し，これをアジュバントに溶解しAFP高値を示す進行肝癌6症例に2週間毎に皮内接種した．AFPの低下や抗腫瘍効果は認められなかったが，テトラマー陽性細胞が増加し，IFNγ ELISPOTが増加したことから，AFPに対する特異的な免疫応答が誘導されることが確認された．彼らはまた10例の進行肝癌症例に，これらのペプチドをパルスした自己DCを2週間毎に接種した[32]．やはり半数以上の症例においてAFP反応性のT細胞の増加とIFNγ ELISPOTの増加をみたと報告している．現時点ではペプチドを用いたこのような治療で明らかな抗腫瘍効果は観察されていない.

むすび

肝癌に対する免疫治療への期待は高いが，明確な治療効果をもつ治療法はいまだ確立されていない．進行肝癌に対してはIFNαを併用した化学療法が有用である可能性があるが，単独で有用性が示された免疫治療法はない．免疫モニタリングシステムを用いて，特異的な免疫応答がどの程度誘導されるかなどの検討を加えて，今後治療法の改良を図っていく必要がある．治療後のアジュバントとしてはIFN治療をはじめ，腫瘍ワクチン治療や養子免疫治療がある一定の効果をもつ可能性があると考えられる.

文献

1) Butterfield LH. Immunotherapeutic strategies for hepatocellular carcinoma. Gastroenterology. 2004; 127: S232-S241.
2) Palmer DH, Hussain SA, Johnson PJ. Gene- and immunotherapy for hepatocellular carcinoma. Expert Opin Biol Ther. 2005; 5: 507-23.
3) Avila MA, Berasain C, Sangro B, et al. New therapies for hepatocellular carcinoma. Oncogene. 2006; 25: 3866-84.
4) Llovet JM, Sala M, Castells L, et al. Randomized controlled trial of interferon treatment for advanced hepatocellular carcinoma. Hepatology. 2000; 31: 54-8.
5) Kubo S, Nishiguchi S, Hirohashi K, et al. Effects of long-term postoperative interferon-alpha therapy on intrahepatic recurrence after resection of hepatitis C virus-related hepatocellular carcinoma. A randomized, controlled trial. Ann Intern Med. 2001; 134: 963-7.
6) Urabe T, Kaneko S, Matsushita E, et al. Clinical pilot study of intrahepatic arterial chemotherapy with methotrexate, 5-fluorouracil, cisplatin and subcutaneous interferon-alpha-2b for patients with locally advanced hepatocellular carcinoma. Oncology. 1998; 55: 39-47.
7) Yin X, Lu M, Liang L, et al. Systemic chemo-immunotherapy for advance-stage hepatocellular carcinoma. World J Gastroenterol. 2005; 11: 2526-9.
8) Yeo W, Mok TS, Zee B, et al. A randomized phase III study of doxorubicin versus cisplatin/interferon α-2b/doxorubicin/fluorouracil (PIAF) combination chemotherapy for unresectable hepatocellular carcinoma. J Natl Cancer Inst. 2005; 97: 1532-8.
9) Sakon M, Nagano H, Dono K, et al. Combined intraarterial 5-fluorouracil and subcutaneous interferon-alpha therapy for advanced hepatocellular carcinoma with tumor thrombi in the major portal branches. Cancer. 2002; 94: 435-42.
10) Ota H, Nagano H, Sakon M, et al. Treatment of hepatocellular carcinoma with major portal vein thrombosis by combined therapy with subcutaneous interferon-alpha and intra-arterial

5-fluorouracil; role of type I interferon receptor expression. Br J Cancer. 2005; 93: 557-64.
11) Obi S, Yoshida H, Toune R, et al. Combination therapy of intraarterial 5-fluorouracil and systemic interferon-alpha for advanced hepatocellular carcinoma with portal venous invasion. Cancer. 2006; 106: 1990-7.
12) Takehara T, Uemura A, Tatsumi T, et al. Natural killer cell-mediated ablation of metastatic liver tumors by hydrodynamic injection of IFNα gene to mice. Int J Cancer (in press).
13) Lygidakis NJ, Kosmidis P, Ziras N, et al. Combined transarterial targeting locoregional immunotherapy-chemotherapy for patients with unresectable hepatocellular carcinoma: a new alternative for an old problem. J Interferon Cytokine Res. 1995; 15: 467-72.
14) Reinisch W, Holub M, Katz A, et al. Prospective pilot study of recombinant granulocyte-macrophage colony-stimulating factor and interferon-gamma in patients with hepatocellular carcinoma. J Immunother. 2002; 25: 489-99.
15) Rosenberg SA, Lotze MT, Muul LM, et al. A progress report on the treatment of 157 patinets with advanced cancer using lymphokine-activated killer cells and interleukin-2 or high-dose interleukin-2 alone. N Engl J Med. 1987; 316: 889-97.
16) Matsuda H, Takehara T, Naito M, et al. Adoptive immunotherapy for the treatment of patients with hepatocellular carcinoma. Acta Hepatologica Japonica. 1990; 31: 428-34.
17) Takayama T, Sekine T, Makuuchi M, et al. Adoptive immunotherapy to lower postsurgical recurrence rates of hepatocellular carcinoma: a randomised trial. Lancet. 2000; 356: 802-7.
18) Takeda T, Watanabe M, Umeshita K, et al. Long-term prognosis of hepatocellular carcinoma patients treated with adoptive immunotherapy. Jpn J Cancer Chemother. 2004; 31: 1646-8.
19) Sakakibara M, Kanto T, Inoue M, et al. Quick generation of fully mature dendritic cells from monocytes with OK432, low-doseprostanoid and interferon-α as potent immune enhancers. J Immunother. 2006; 29: 67-77.
20) Ladhams A, Schmidt C, Sing G, et al. Treatment of non-resectable hepatocellular carcinoma with autologous tumor-pulsed dendritic cells. J Gastroenterol Hepatol. 2002; 17: 889-96.
21) Iwashita Y, Tahara K, Goto S, et al. A phase I study of autologous dendritic cell-based immunotherapy for patients with unresectable primary liver cancer. Cancer Immunol Immunother. 2003; 52: 155-61.
22) Stift A, Friedl J, Dubsky P, et al. Dendritic cell-based vaccination in solid cancer. J Clin Oncol. 2003; 21: 135-42.
23) Tatsumi T, Takehara T, Kanto T, et al. Administration of interleukin-12 enhances the therapeutic efficacy of dendritic cell-based tumor vaccines in mouse hepatocellular carcinoma. Cancer Res. 2001; 61: 7563-7.
24) Mazzolini G, Alfaro C, Sangro B, et al. Intratumoral injection of dendritic cells engineered to secrete interleukin-12 by recombinant adenovirus in patients with metastatic gastrointestinal carcinomas. J Clin Oncol. 2005; 23: 999-1010.
25) Feijoo E, Alfaro C, Mazzolini G, et al. Dendritic cells delivered inside human carcinomas are sequestered by interleukin-8. Int J Cancer. 2005; 116: 275-81.
26) Mizukoshi E, Nakamoto Y, Tsuji H, et al. Identification of α-fetoprotein-derived peptides recognized by cytooxic T lymphocytes in HLA-A24$^+$ patients with hepatocellular carcinoma. Int J Cancer. 2006; 118: 1194-204.
27) Bricard G, Bouzourene H, Martinet O, et al. Natirally acquired MAGE-A10- and SSX-2-specific CD8$^+$ T cell responses in patients with hepatocellular carcinoma. J Immunol. 2005; 174: 1709-16.
28) Shang XY, Chen HS, Zhang HG, et al. The spontaneous CD8$^+$ T-cell response to HLA-A2-restricted NY-ESO-1b peptide in hepatocellular carcinoma patients. Clin Cancer Res. 2004; 10: 6946-55.
29) Komori H, Nakatsura T, Senju S, et al. Identification of HLA-A2- or HLA-A24-restricted CTL epitopes possibly useful for glypican-3-specific immunotherapy of hepatocellular carcinoma. Clin Cancer Res. 2006; 12: 2689-97.
30) Kuang M, Peng BG, Lu MD, et al. Phase II randomized trial of autologous formalin-fixed tumor vaccine for postsurgical recurrence of

hepatocellular carcinoma. Clin Cancer Res. 2004; 10: 1574-9.

31) Butterfield LH, Ribas A, Meng WS, et al. T-cell responses to HLA-A*0201 immunodominant peptides derived from α-fetoprotein in patients with hepatocellular cancer. Clin Cancer Res. 2003; 9: 5902-8.

32) Butterfield LH, Ribas A, Dissette VB, et al. A phase I/II trial testing immunization of hepatocellular carcinoma patients with dendritic cells pulsed with four alpha-fetoprotein peptides. Clin Cancer Res. 2006; 12: 2817-25.

Available online at www.sciencedirect.com

SCIENCE DIRECT®

Genomics 84 (2004) 867–875

GENOMICS

www.elsevier.com/locate/ygeno

Genome-wide transcriptome mapping analysis identifies organ-specific gene expression patterns along human chromosomes

Taro Yamashita[a], Masao Honda[a], Hajime Takatori[a], Ryuhei Nishino[a], Nobuaki Hoshino[b], Shuichi Kaneko[a,*]

[a]*Department of Cancer Gene Regulation, Kanazawa University Graduate School of Medical Science, 13-1 Takara-Machi, Kanazawa 920-8641, Japan*
[b]*Faculty of Economics, Kanazawa University, Kakuma-Machi, Kanazawa 920-1192, Japan*

Received 31 March 2004; accepted 6 August 2004
Available online 26 August 2004

Abstract

The Human Genome Project has revealed that there about 32,000 protein-encoding genes, which are distributed throughout the genome. It is unclear, however, whether genes are distributed on the chromosomes according to patterns linked to organ specificity. To explore the relationship between genes actively transcribed in normal tissues and their chromosomal locations, we analyzed serial analysis of gene expression libraries of normal human liver, brain, breast, and colon tissues. Transcriptome mapping analysis revealed that transcriptional activity in each tissue varied according to the chromosomal domains, and a weak positive correlation was observed between transcription density and gene density. We identified six liver-related and five colon-related chromosomal domains highly transcribed in each tissue, whereas no brain-related or breast-related chromosomal domains were identified. Representative genes located on these chromosomal domains were associated with the function of each organ and were highly conserved in both mouse and rat genomes. These data revealed that the transcriptional activities of normal human tissues are well orchestrated at chromosomal levels, suggesting that highly expressed genes may share physical proximity.
© 2004 Elsevier Inc. All rights reserved.

Keywords: Genomics; Gene expression profiling; Serial analysis of gene expression; Transcriptome mapping; Organ-related chromosomal domain

Introduction

Analysis of the human genome has shown that there are about 32,000 protein-coding genes distributed throughout the 46 chromosomes. Previous work, however, indicated that the highly expressed genes in all human tissues are clustered in several chromosomal domains [1]. In the nematode *Caenorhabditis elegans*, genes expressed in the muscle are clustered in small groups along the chromosomes [2], suggesting a relationship between muscle-specific functionality and chromosomal domains actively transcribed in *C. elegans*. Another report revealed that groups of adjacent genes were coregulated in the fly *Drosophila melanogaster*, suggesting that coregulated genes also share physical proximity in *D. melanogaster* [3]. Furthermore, a comparative analysis of the genomes of *D. melanogaster*, *C. elegans*, and *Saccharomyces cerevisiae* revealed the existence of a "core proteome" highly conserved in yeast, worm, and fly [4], suggesting the heredity of fundamental genomic or proteomic organization associated with the cellular processes or functions commonly observed in all eukaryotes. From these reports, we postulated a hypothesis that the distribution of genes along human chromosomes may exhibit a higher level of organization, which may be linked to organ-specific functionality and conserved in mammals.

To explore the relationship between genes actively transcribed in normal human tissues and chromosomal domains, we analyzed serial analysis of gene expression (SAGE) libraries derived from normal human liver, brain,

* Corresponding author. Fax: +81 76 234 4250.
E-mail address: skaneko@medf.m.kanazawa-u.ac.jp (S. Kaneko).

0888-7543/$ - see front matter © 2004 Elsevier Inc. All rights reserved.
doi:10.1016/j.ygeno.2004.08.008

breast, and colon tissues with human genome sequence information. We observed organ-specific gene expression patterns along the chromosomes in each tissue, identifying six liver-related chromosomal domains and five colon-related chromosomal domains. We found that transcriptional activity in normal human tissues is well orchestrated at the chromosomal level, suggesting that most of the highly expressed genes in each organ might be clustered. We further observed that representative genes located on these chromosomal domains were associated with organ-specific function, and the genes were also clustered on the *Rattus norvegicus* and *Mus musculus* genomes. These findings may be the results of binding of specific transcription factors onto specific chromosomal domains in each tissue or of chromosome rearrangements during mammalian evolution.

Results

Organ-specific gene expression patterns along the chromosome

An outline of the construction of the transcriptome map is shown in Fig. 1. We assigned 27,402 NCBI RefSeq genes (build 31) to 17,193 Locus ID clusters. All SAGE tags detected could be assigned to a total of 55,612 reliable UniGene clusters using the SAGEmap reliable tag-to-gene mapping table (http://www.sagenet.org/SAGEDatabases/unigene.htm). All SAGE tags assigned were related to the Locus ID clusters by UniGene ID, and the origins of the start sites in all genes were mapped to the SAGE tag.

When we investigated the correlation between the number of genes and the number of transcripts in each chromosome using a 5-Mb window moving along the chromosome at 1-Mb intervals, we found that Pearson's correlation coefficients ranged from 0.119 to 0.869 in the liver, 0.107 to 0.838 in the brain, 0.314 to 0.791 in the breast, 0.206 to 0.872 in the colon, and 0.304 to 0.883 in the reference library (Table 1). These data suggested that the transcriptional activity in each tissue varied and was not in accordance with the number of genes encoded by each chromosome. The strongest positive correlations, however, were observed in the reference libraries, indicating that gene expression levels in total tissues could be relatively correlated with the number of genes per chromosome.

To investigate the transcription density along the human chromosomes using digital gene expression data, we calculated transcription density factor (TDF), which would be well correlated with the abundance of transcripts and adjusted by gene density in each chromosomal domain, as described under Materials and methods. When we calculated the gene density and TDF in each tissue on whole chromosomal domains, we found that gene expression levels fluctuated along the chromosome, with most genes in most chromosomal domains expressed at a range of $0.5 < TDF < 1.5$ in each tissue (representative transcriptome maps are shown in Fig. 2). Gene expression patterns in each of

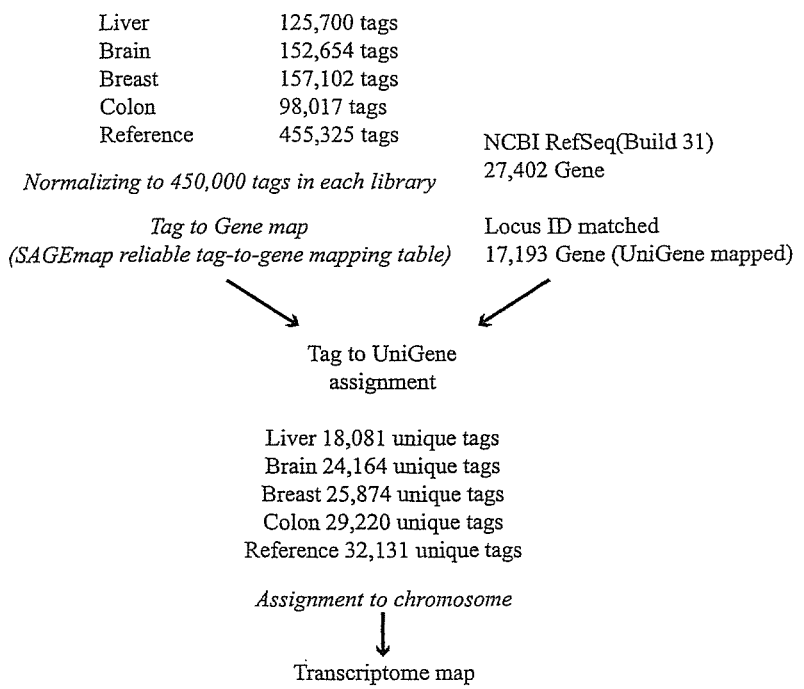

Fig. 1. Schematic outline of transcriptome map construction. All detected SAGE tags were assigned to a total of 55,612 reliable UniGene clusters and related to the Locus ID clusters by UniGene ID. Location of the SAGE tags on the chromosome was coordinated with physical distance information.

Table 1
Correlation between the number of transcripts and the number of genes in each chromosome

Chromosome	Liver	Brain	Breast	Colon	Reference
1	0.483	0.674	0.640	0.537	0.703
2	0.491	0.739	0.642	0.670	0.675
3	0.517	0.672	0.594	0.538	0.739
4	0.404	0.470	0.512	0.391	0.512
5	0.869	0.785	0.669	0.721	0.883
6	0.720	0.838	0.709	0.805	0.856
7	0.638	0.686	0.568	0.699	0.670
8	0.324	0.386	0.314	0.335	0.364
9	0.355	0.776	0.555	0.705	0.515
10	0.448	0.498	0.322	0.441	0.304
11	0.224	0.801	0.544	0.556	0.778
12	0.397	0.632	0.711	0.616	0.730
13	0.281	0.398	0.478	0.311	0.459
14	0.354	0.573	0.378	0.431	0.651
15	0.119	0.284	0.345	0.206	0.339
16	0.520	0.719	0.500	0.588	0.666
17	0.410	0.550	0.791	0.670	0.634
18	0.211	0.107	0.453	0.359	0.364
19	0.587	0.701	0.555	0.610	0.700
20	0.570	0.769	0.701	0.673	0.709
21	0.766	0.627	0.547	0.872	0.744
22	0.429	0.563	0.680	0.445	0.593
X	0.653	0.786	0.747	0.705	0.758
Average	0.468	0.610	0.563	0.560	0.624

these chromosomal domains were tissue specific, indicating the existence of distinct, organ-specific gene expression patterns along the chromosomes.

Identification of organ-related chromosomal domains

To determine whether each tissue type had distinct gene expression patterns along the chromosomes, we mathematically classified the chromosomal domains by TDF. For each tissue type, we determined if the TDF in a given SAGE library exceeded 1.8 and if the TDF in the other libraries was less than 1.0. The chromosomal domains identified by these criteria fulfilled the condition that gene expression levels in the given tissue were increased more than 6-fold compared with those of other tissues and that gene expression levels in the other tissues did not exceed the 2.7-fold of the reference levels. To diminish the effect of a gene highly expressed in a chromosomal domain of low gene density on a TDF score, we selected chromosomal domains more than 3 Mb long, containing more than two genes in a window of 1 Mb, with TDF >1.8 consecutively.

Using these criteria, we first compared the gene expression patterns of the liver. Using SAGE libraries derived from normal liver and a mixture of five normal livers, we investigated whether there were individual variations in hepatic gene expression patterns along the chromosome. The TDF derived from the normal liver SAGE library could be correlated with the TDF derived from the mixture of five normal liver SAGE libraries, with Pearson's correlation coefficient ranging from 0.618 to 0.960. In addition, the difference between the TDF in the normal liver library and that in the pooled liver library never exceeded 1.8 on all chromosomal domains (data not shown), indicating that there were no individual differences of more than sixfold along the chromosome. These data also suggested that the criteria used here could enable us to disregard the individual variations in gene expression patterns and could be useful for identifying chromosomal domains actively transcribed in each tissue type.

We investigated whether highly expressed genes clustered along the chromosome in each tissue and applied the criteria to the mapping data of the liver, brain, breast, and colon SAGE libraries. After filtering transcriptome mapping data of the liver, we found that genes highly expressed in the liver were clustered in six chromosomal domains, compared with the brain, breast, and colon libraries. Similarly, we identified five colon-related chromosomal domains, but no brain-related or breast-related chromosomal domains.

To rule out the possibility of chance observation of high variance in the selected domains, we performed a permutation test as described under Materials and methods. The identified liver-related chromosomal domains and colon-related chromosomal domains were fully significant (liver-related chromosomal domains $p < 0.0001$, colon-related chromosomal domains $p < 0.0001$), revealing the statistical validity of our criteria.

Representative transcriptome mapping data and chromosomal domains are shown in Fig. 2 (chromosomes 1 and 6). Cytogenetically, we found liver-related chromosomal domains at 1q23–q25, 4q21–q24, 6p12.1, 11q23–q24, 17q11, and 18q12; we found colon-related chromosomal domains at 2p21, 3q23, 8q21, 12q15, and 21q22.

The numbers of SAGE tags distributed in each organ-related chromosomal domain are shown in Table 2. In liver-related chromosomal domains, the average gene expression levels in the liver were increased 18.1-, 22.2-, and 22.5-fold compared with levels in the brain, breast, and colon, respectively. In colon-related chromosomal domains, the average gene expression levels in the colon were increased 15.0-, 13.3-, and 8.0-fold compared with levels in the liver, brain, and breast, respectively.

Conservation of the organ-related chromosomal domains in human and rodent genomes

To examine whether organ-related chromosomal domains were preserved in other mammalian genomes, we investigated the possible homologous genes and their locations on the *R. norvegicus* and *M. musculus* genomes using the HomoloGene database. Of 412 human genes comprising 11 organ-related chromosomal domains, we identified 213 rat homologous genes (51.7%) and 230 mouse homologous genes (55.8%). Almost all of the homologous genes on human chromosomes 1q23–q25, 2p21, 3q23, 4q21–q24, 11q23, 12q15, 17q11, 18q12.1, and Xq21.3–q22 were located on the same chromosomal

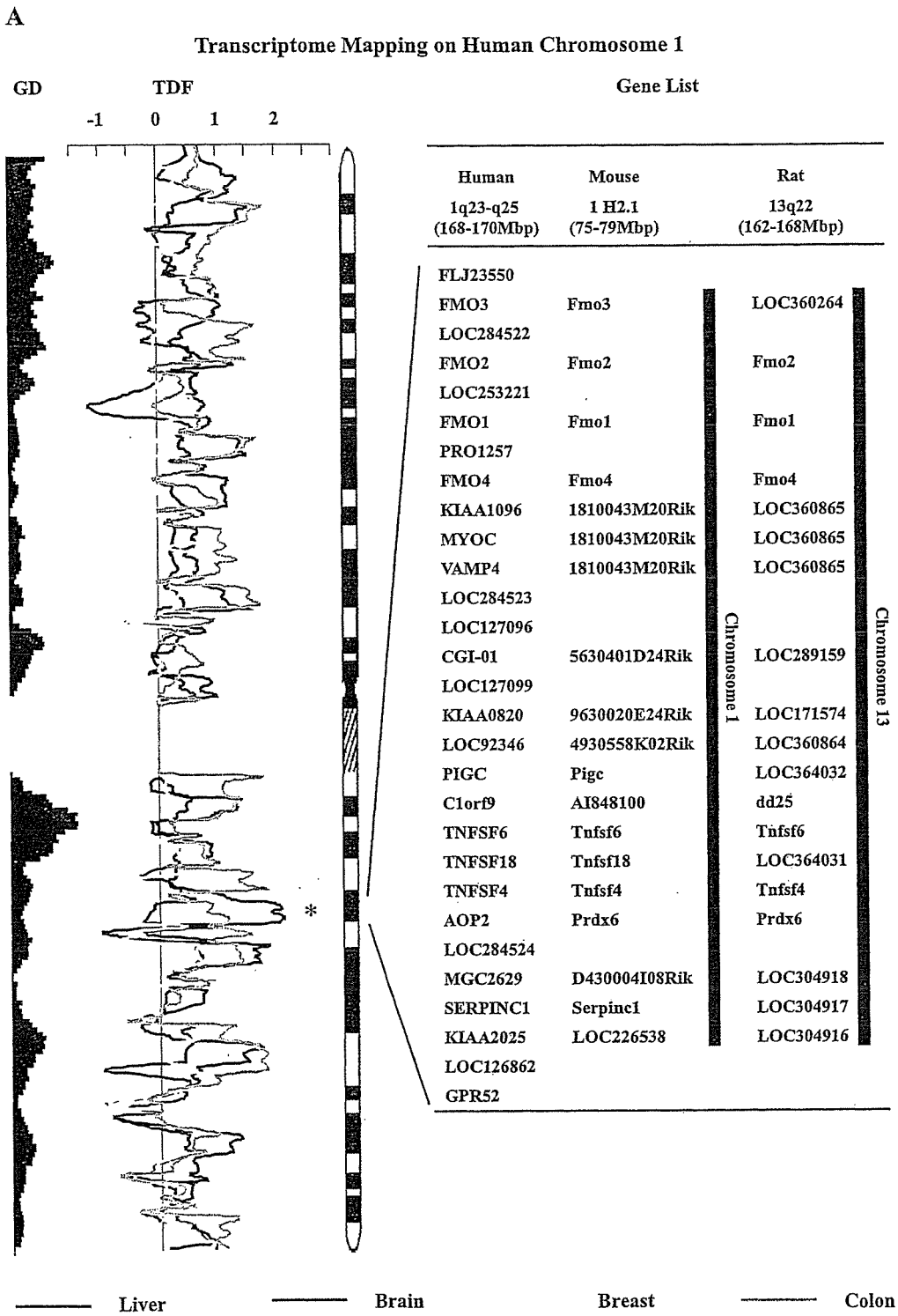

Fig. 2. Representative transcriptome map analysis of liver, brain, breast, and colon SAGE libraries. Differential expression patterns were observed in each tissue along the chromosome, and asterisks indicate the organ-related chromosomal domain. The genes located on the organ-related chromosomal domain in human are shown. Their possible homologous genes on mouse and rat genome are also shown.

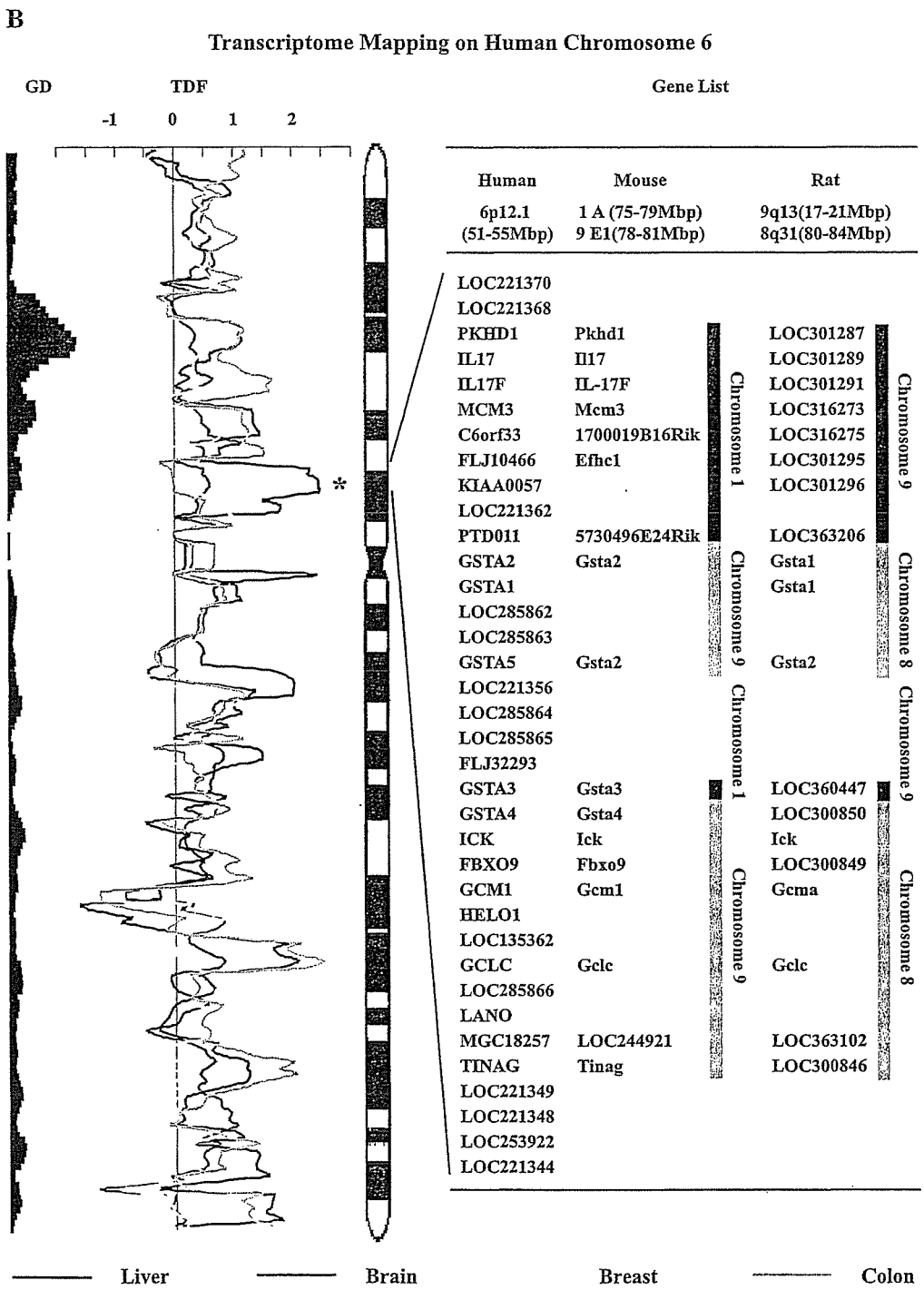

Fig. 2 (*continued*).

domains of the mouse and rat genomes (representative data of human 1q23–q25, mouse 1H2.1, and rat 13q22 are shown in Fig. 2). However, genes on chromosomes 6p12.1 and 21q22 were located on two different chromosomal domains of the rat and mouse genomes (representative data of human 6p12.1, mouse 1A and 9E1, and rat 9q13 and 8q31 are shown in Fig. 2). Interestingly, more than half of these chromosomal domains (1q23–q25, 4q21–q24, 6p12.1, 11q23, 18q12.1, and 21q22) contained multigene families. These data revealed that most of organ-related chromosomal domains identified here are conserved in the human and rodent genomes, which might have originated from chro-

Table 2
Cytogenetic loci of gene clusters highly expressed in each organ

Cytogenetic locus	Liver	Brain	Breast	Colon	Reference
Liver-related chromosomal domains					
1q23–q25	1,326	140	169	326	370
4q21–q25	2,104	132	139	129	352
6p12.1	983	189	166	84	210
11q23.1–q23.2	30,168	932	840	804	3552
17q11	3,329	777	445	385	778
18q12.1	1,752	26	26	28	168
Total	39,662	2196	1785	1756	5430
Colon-related chromosomal domains					
2p21	40	72	127	411	154
3q22–q23	59	55	86	406	116
8q13–q22.1	62	32	49	531	139
12q14.1–q21.1	35	37	53	510	132
21q22.3	25	52	100	1447	265
Total	221	248	415	3305	806

mosomal rearrangement and/or gene duplication during mammalian evolution (supplementary figure of all transcriptome mapping data and the gene list are available on our home page: http://www.intmedkanazawa.jp/).

Analysis of gene function on organ-related chromosomal domains

We investigated the functions of genes clustered on organ-related chromosomal domains using the Gene Ontology database (http://www.geneontology.org/). We could retrieve the information for 227 of 412 clustered genes from the Gene Ontology database, and 150 of these were annotated by molecular function. Interestingly, 74 of 150 genes were associated with metabolic enzymes, revealing that about half of the genes clustered on organ-related chromosomal domains are those encoding metabolic enzymes, suggesting the close relation of the chromosomal domains and some metabolic processes.

We searched the downstream targets of the genes on the organ-related chromosomal domains using PathwayAssist software and investigated the common targets and functions of the genes on the chromosomal domains. As shown in Table 3, 10 of 11 organ-related chromosomal domains consisted of genes associated with common metabolic or functional pathways, whereas no common targets were detected on chromosome 12q15 (colon-related chromosomal domain). Apparently, gene families associated with metabolism are clustered in liver-related chromosomal domains, such as 6p12.1 with xenobiotic metabolism, 4q21–q24 with alcohol and aldehyde metabolism, and 11q23–q24 with lipid metabolism. On the other hand, genes associated with transporters and apoptosis were clustered in colon-related chromosomal domains, such as 8q21 with anion transporter and 21q22 with apoptosis and cell proliferation. These data suggested that the genes clustered on organ-related chromosomal domains might be associated with the organ-specific functionality.

Discussion

The release of the sequence of the entire human genome and the development of advanced gene expression profiling technologies have focused interest on understanding the relationship between gene expression and chromosomal organization in complex systems. The genome is not simply a patchwork of genes but forms complex structures. The presence of chromosomal regions enriched in gene families has been demonstrated for several gene clusters. For example, the major histocompatibility complex is located on chromosome 6p21 [5], and the apolipoproteins are located on chromosome 11q23 [6]. It is not known, however, if genes abundantly expressed in each organ are distributed throughout the genome or clustered on various chromosomes. This question was addressed by assessing the chromosomal distribution of genes expressed in the brain and heart using EST collection databases [7,8]. Although these studies reported complex tissue-specific gene regulation patterns in the brain and heart, organ-specific gene expression patterns have not been compared simultaneously in several tissues. In addition, since EST databases are not generated according to the same methods by each distributor, comparison of the expression levels between organs may not be accurate. In this study, therefore, we utilized SAGE analysis to obtain unbiased gene expression data from hundreds of thousands of transcripts expressed in the normal human liver, brain, breast, and colon. Using genome-wide transcriptome maps for each organ, we identified six liver-related and five colon-related chromosomal domains. Thus, it seemed that organ-specific genes are accumulated on specific chromosomal domains for each organ.

Table 3
Functional annotation of the genes located on organ-related chromosomal domains

Cytogenetic locus	Function
Liver-related chromosomal domains	
1q23–q25	Xenobiotic mono-oxygenation; apoptosis and cell proliferation
4q21–q25	Alcohol and formaldehyde metabolism
6p12.1	Xenobiotic metabolism
11q23.1–q23.2	Lipid metabolism
17q11	Amyloid production
18q12.1	Focal contact; apoptosis and cell proliferation
Colon-related chromosomal domains	
2p21	Apoptosis and cell proliferation
3q22–q23	Ion transporter; apoptosis and cell proliferation
8q13–q22.1	Ion transporter; apoptosis and cell cycle regulation
12q14.1–q21.1	None
21q22.3	Apoptosis and cell proliferation; mucin production